

lin-35/Rb* and *ubc-18*, an E2 ubiquitin-conjugating enzyme, function redundantly to control pharyngeal morphogenesis in *C. elegans

David S. Fay^{1,*}, Edward Large¹, Min Han² and Monica Darland¹

¹Department of Molecular Biology, University of Wyoming, PO Box 3944, Laramie, WY 82071-3944, USA

²Howard Hughes Medical Institute and Department of Molecular, Cellular, and Developmental Biology, University of Colorado, Boulder, CO 80309-0347, USA

*Author for correspondence (e-mail: davidfay@uwyo.edu)

Accepted 24 April 2003

SUMMARY

The retinoblastoma gene product has been implicated in the regulation of multiple cellular and developmental processes, including a well-defined role in the control of cell cycle progression. The *Caenorhabditis elegans* retinoblastoma protein homolog, LIN-35, is also a key regulator of cell cycle entry and, as shown by studies of synthetic multivulval genes, plays an important role in the determination of vulval cell fates. We demonstrate an additional and unexpected function for *lin-35* in organ morphogenesis. Using a genetic approach to isolate *lin-35* synthetic-lethal mutations, we have identified redundant roles for *lin-35* and *ubc-18*, a gene that encodes an E2

ubiquitin-conjugating enzyme closely related to human UBCH7. *lin-35* and *ubc-18* cooperate to control one or more steps during pharyngeal morphogenesis. Based on genetic and phenotypic analyses, this role for *lin-35* in pharyngeal morphogenesis appears to be distinct from its cell cycle-related functions. *lin-35* and *ubc-18* may act in concert to regulate the levels of one or more critical targets during *C. elegans* development.

Key words: *lin-35*, Retinoblastoma, *ubc-18*, Ubiquitin, *C. elegans*, Pharynx

INTRODUCTION

Functional disruption of the retinoblastoma gene product (pRb) has been implicated as a causal event in the genesis of a wide range of human cancers (reviewed by Sherr, 1996; Nevins, 2001). pRb and its structurally related family members, p107 and p130, play key roles in the regulation of several fundamental cellular processes, including cell cycle entry and the induction of apoptosis (reviewed by Kaelin, 1999; Morris and Dyson, 2001). The ability of pRb to regulate these events is linked directly to its activity as a transcriptional repressor. Specifically, pRb binds to E2F family members and inhibits the expression of E2F target genes (reviewed by Dyson, 1998; Harbour and Dean, 2000). These targets include positive-acting cell cycle regulators, such as cyclins E and A (DeGregori et al., 1995; Duronio and O'Farrell, 1995; Ohtani et al., 1995; Schulze et al., 1995), genes that are required for DNA synthesis (Dou et al., 1994; DeGregori et al., 1995), and mediators of apoptosis (DeGregori et al., 1997; Hsieh et al., 1997; Tsai et al., 1998). pRb transcriptional repression of E2F targets occurs through a number of distinct mechanisms, many of which involve the recruitment of enzymes that modify chromatin structure. These include histone deacetylase (Brehm et al., 1998; Luo et al., 1998; Magnaghi-Jaulin et al., 1998), members of the nucleosome remodeling complex (Dunaief et al., 1994; Strober et al., 1996; Zhang et al., 2000) and proteins required for histone methylation (Nielsen et al., 2001).

In addition to cell-cycle regulation, in vitro and tissue culture studies have shown that pRb associates with a diverse set of proteins, many of which regulate the expression of genes required for tissue-specific differentiation (reviewed by Morris and Dyson, 2001). For example, pRb enhances the DNA binding and transactivation activities of NF-IL6 (Chen et al., 1996b) and the C/EBP (Chen et al., 1996a) family of transcription factors to promote adipocyte and leukocyte differentiation, respectively. pRb also promotes muscle differentiation by augmenting the activity of MyoD (Gu et al., 1993) and through inhibition of the transcriptional repressor HBP1 (Tevosian, 1997; Shih et al., 1998). Finally, pRb may bind and regulate the activities of a number of additional factors, including the paired homeodomain-containing proteins Pax3, Pax5, Chx10 and Mhox (Wiggin et al., 1998; Eberhard and Busslinger, 1999); several hormone-responsive transcription factors, including the glucocorticoid receptor (Singh et al., 1995); and the osteoblast transcription and differentiation factor, CBFA1 (Thomas et al., 2001). Whether or not the majority of these reported activities represent authentic in vivo functions for *Rb* remains to be determined.

Acting in concert with transcriptional regulatory factors, the ubiquitin-mediated degradation pathway has emerged as the other principal mechanism by which cells control the abundance of individual proteins. The process is carried out by three classes of enzymes (termed E1, E2 and E3) that act sequentially to catalyze the attachment of ubiquitin, a highly

conserved ~76 amino acid protein, to the protein substrate targeted for degradation (reviewed by Weissman, 2001). The process is initiated by E1 enzymes (also known as ubiquitin-activating enzymes), which form a thiol-ester bond with the C-terminal glycine of ubiquitin in an ATP-dependent manner. The E2 or UBC (for ubiquitin-conjugating or ubiquitin-carrier) enzyme then accepts ubiquitin from the E1 via a trans-thiolation reaction involving the C terminus of ubiquitin. Finally, the transfer of ubiquitin from E2 to a lysine on the target protein is catalyzed by the E3 ubiquitin ligase. E3 enzymes can further be subdivided into two separate families containing either a HECT or a RING finger domain. E3s with a HECT domain form thiol-ester intermediates with ubiquitin prior to attachment to the target protein (Huibregtse et al., 1995), whereas E3s with a RING finger mediate the direct transfer of ubiquitin from E2 to the target protein (Joazeiro and Weissman, 2000). In either case, the majority of ubiquitylated proteins are subsequently degraded by the 26S proteasome.

A recent analysis of the *C. elegans* genome identified 20 genes encoding predicted E2/UBC enzymes along with three UBC variants (Jones et al., 2002). This compares with 12 UBCs in *S. cerevisiae*, 25 in *Drosophila* and 26 that have thus far been identified in the human proteome. Thus, complexity in the ubiquitylation process begins at the level of UBCs and is further amplified by the large number of potential E3 genes found in the genomes of most higher eukaryotes; the *C. elegans* genome encodes for >150 RING-finger or HECT domain proteins. Interestingly, RNA-mediated interference (RNAi) experiments of the 23 *C. elegans* UBC genes revealed functions for only four of them (Jones et al., 2002). RNAi of these genes [*let-70 (ubc-2)*, *ubc-9*, *ubc-12*, and *ubc-14*], all of which are conserved in yeast, results in developmental arrest at various stages. Thus, a large proportion of UBCs in *C. elegans* may be functionally redundant, either with each other or with other cellular factors that act to regulate protein levels.

Using a genetic screen to identify mutations causing synthetic phenotypes with *lin-35/Rb* in *C. elegans*, we have previously reported the identification of mutations in *fzr-1*, a regulatory subunit of the APC proteasome (Fay et al., 2002). *lin-35; fzr-1* double mutants display a hyperproliferation phenotype that affects virtually all cell types examined. We now describe our analysis of another mutation identified in this screen. Cloning of the gene reveals that it corresponds to *ubc-18*, the *C. elegans* homolog of human UBCH7 (ARIH1 – Human Gene Nomenclature Database). The coordinate inactivation of *lin-35* and *ubc-18* leads to several developmental defects, including a failure to execute pharyngeal morphogenesis properly. The expanding role of *lin-35* beyond cell-cycle control and vulval induction in *C. elegans* should shed light on the conserved role of Rb in higher eukaryotes.

MATERIALS AND METHODS

Strains and genetic methods

Maintenance, culturing, and genetic manipulations of *C. elegans* were carried out according to standard procedures at 20°C (Sulston and Hodgkin, 1988). Strains used in the phenotypic analysis included WY43 [*ubc-18(ku354)*], WY83 [*lin-35; ubc-18; kuEx119*], WY78 [*lin-35; dpy-17(e164), ubc-18(ku354); unc-32(e189); kuEx119*],

MH1834 [*ubc-18(ku354), unc-32*], SM469(*pha-4::GFP-NLS*), SM481(*pha-4::GFP-mem*), MH1384 (*ajm-1::GFP*), PD4792 (*myo-2::GFP*) and DP132 (*unc-119::GFP*).

Strains used to map *ubc-18(ku354)* included: *lin-35(n745); dpy-17(e164), unc-32(e189)III* [6/19 Unc-non-Dpy (UND) and 9/12 Dpy-non-Unc (DNU) recombinants picked up the *ubc-18* mutation]; and *lin-35(n745); sma-3(e491), unc-32(e189)* [16/16 UNS and 0/7 SNU picked up the *ubc-18* mutation]. Strains WY2 [*dpy-17(e164), ubc-18(ku354); unc-32(e189)*], WY78 and CB4856 were used in SNP mapping procedures to place *ubc-18(ku354)* between SNP markers *eam34f12.s1@151* on cosmid R01H2 and *eam49b07.s1@287* on cosmid T21D11. For this effort, a total of 98 DNU and UND recombinants were isolated, homozygosed and (in the case of recombinants derived from WY2) injected with *lin-35* dsRNA to ascertain the status of the *ubc-18* mutation. For SNP mapping with WY78, we used a *lin-35* strain that had been backcrossed five times to CB4856 (WY72) and followed the presence of *ubc-18* based on the requirement for *kuEx119*. For additional details on genetic mapping, see Fay et al. (Fay et al., 2002).

Duplication and deficiency analysis

lin-35; ubc-18/ubc-18; qDp3 animals were generated by crossing JK867 [*dpy-17(e164) ncl-1(e1865) unc-36(e251)III; qDp3(III;f)*] hermaphrodites to *lin-35* males, then crossing F1 male progeny to *lin-35; ubc-18, unc-32; kuEx119* hermaphrodites. Putative *lin-35; d17, ncl-1, unc-36/ubc-18, unc-32; qDp3* animals were identified, as well as *lin-35; ubc-18; unc-32; qDp3* animals in the next generation. Such animals were wild type and generated UNC-32 but not DPY-17, UNC-36 progeny. The presence of the *lin-35* homozygous mutation was confirmed by the phenotypes of the Unc animals (*lin-35; ubc-18; unc-32*) as well as through the use of *lin-15a(RNAi)* which led to a high penetrance of the Muv phenotype when *lin-35* was homozygous. To generate *lin-35; ubc-18, unc-32/+; qDp3* animals, *lin-35; ubc-18; unc-32; qDp3* animals were crossed to *lin-35; dpy-17, unc-32/+* males and wild-type cross progeny hermaphrodites that gave rise to DpyUnc animals were identified, indicating the genotype *lin-35; ubc-18; unc-32/dpy-17, unc-32; qDp3*. For deficiency mapping, *lin-35; dpy-17, ubc-18, unc-32/+* males were crossed to MT1978 [*nDf16/unc-36(e251) dpy-19(e1259)*] and *lin-35; nDf16/dpy-17, ubc-18, unc-32; kuEx119* animals were identified. However, such animals, when fertile, were rapidly out-competed by homozygous *lin-35; ubc-18; kuEx119* sibling progeny. Similar results were obtained when we attempted to produce animals with the genotype *lin-35; nDf16/+; kuEx119*, suggesting that the *lin-35* mutation may be deleterious in conjunction with the deficiency. Direct testing of *nDf16/+* animals for sensitivity to *lin-35* reduction using RNAi led to first generation *nDf16/+* progeny that were uniformly sterile (data not shown). Thus, our inability to isolate stable *lin-35; ubc-18/nDf16; kuEx119* strains stems from an apparent toxic genetic interaction between *lin-35* and *nDf16*.

Other methods

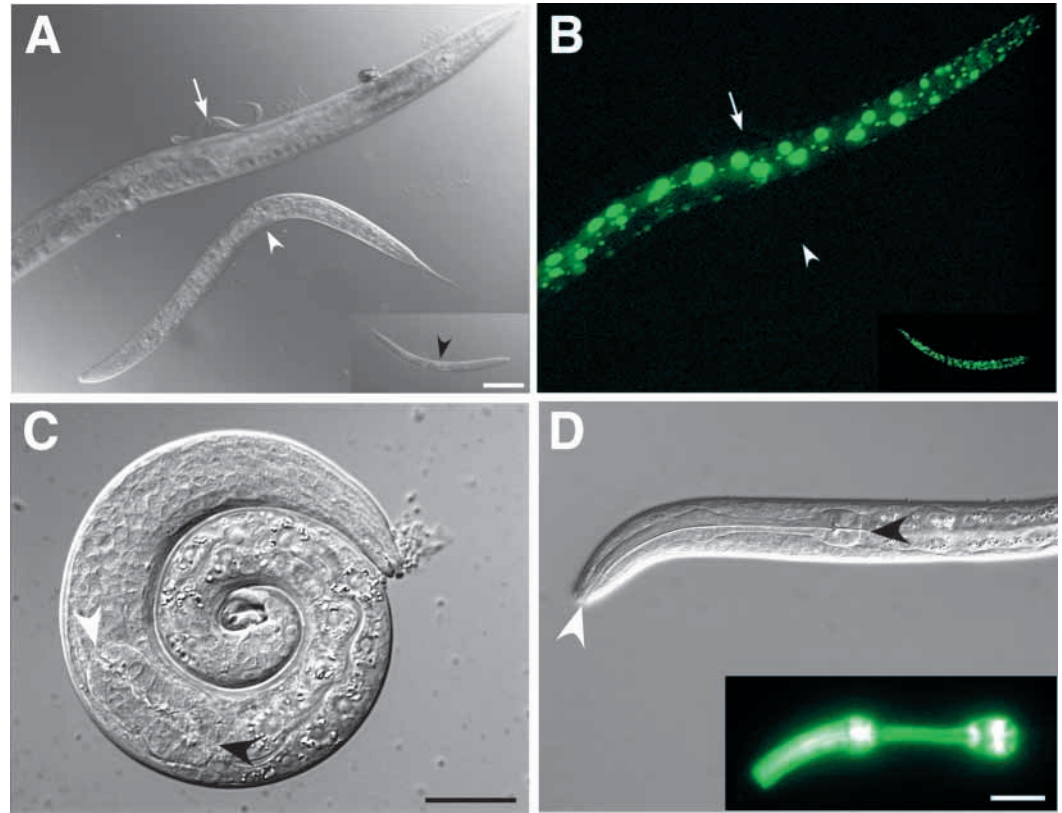
Cosmid rescue

Rescue was obtained by co-injection of *C. elegans* genomic cosmids or PCR products with pRF4 into WY83 using standard procedures (Mello and Fire, 1995). Rescued animals were fertile and showed a roller (Rol) phenotype. For single-gene rescue of WY83 animals, a 2570 bp PCR fragment corresponding to nucleotides 31,220–33,790 of R01H2 was used. The *ubc-18*-coding region spans nucleotides 32,225–32,928 and is encoded by the reverse strand.

RNAi

RNAi was carried out according to standard methods (Fire et al., 1998; Fraser et al., 2000). Feeding vectors were constructed as previously described (Fay et al., 2002). For *lin-37*, a 774 bp fragment of *C. elegans* genomic DNA corresponding to nucleotides 1763–2555 of cosmid ZK418 (261–816 of *lin-37*) was subcloned into the polylinker

Fig. 1. Synergism between mutations in *lin-35* and *ubc-18*. DIC (A) and corresponding GFP fluorescence (B) images. The large adult with GFP fluorescence is of genotype *lin-35; ubc-18; kuEx119*. The white arrows indicate the position of an arrested *lin-35; ubc-18* L1 larva that failed to inherit the array; the white arrowheads indicate a sterile *lin-35; ubc-18* young adult. Inset in A shows an arrested *lin-35; ubc-18; KuEx119* larval-stage animal treated with *lin-35(RNAi)* (same animal is shown in the inset in B). (C,D) L1 animals of genotypes *lin-35; ubc-18* and wild type, respectively. White and black arrowheads indicate anterior and posterior pharyngeal boundaries, respectively. Note the failure of the mutant pharynx to extend to the anterior end of the animal. (Inset in D) *myo-2::GFP* fluorescence in the wild-type background, highlighting the bi-lobed shape of the pharynx. Scale bars: in A, 100 μ m for A,B; in C, 10 μ m for C; in D, 10 μ m for D.



of PD129.36. For *ubc-18*, a 691 bp PCR fragment of *C. elegans* genomic DNA corresponding to nucleotides 32,232-32,923 of R01H2 (the entire *ubc-18* coding region) was subcloned into vector pPD129.36.

RESULTS

ubc-18/slr-5 is synthetically lethal with *lin-35/Rb*

We have previously described a genetic screen in *C. elegans* that leads to the efficient isolation of mutations that are synthetically lethal with *lin-35* (Fay et al., 2002). Briefly, the strategy employs a strain with two attributes: (1) the strain is homozygous for a strong loss-of-function mutation in *lin-35*; and (2) the strain carries a meiotically unstable extrachromosomal array (*kuEx119*) that contains both wild-type *lin-35*-rescuing sequences and a ubiquitously expressed GFP reporter. Because *lin-35* is nonessential, animals that fail to inherit the array are nevertheless viable and can be identified by their absence of GFP expression. After mutagenesis, animals acquiring mutations that are synthetically lethal with *lin-35* are identified by their complete dependence on the array for viability. To date, we have screened ~7000 haploid genomes and have identified 11 Slr mutations (for synthetic with *lin-35/Rb*) that represent at least 10 loci. We describe the identification of *slr-5(ku354)*, which, based on its molecular identity (see below), we refer to as *ubc-18*.

lin-35; ubc-18; kuEx119 animals are healthy, fertile and generally appear indistinguishable from wild-type animals (Fig. 1A,B). By contrast, most *lin-35; ubc-18* animals that fail

to inherit the array arrest or die as larvae, and those animals reaching adulthood are typically small and sterile (Fig. 1A,B; Table 1). As predicted for a synthetically lethal mutation, inactivation of *lin-35* (expressed from the extrachromosomal array) using RNAi caused *lin-35; ubc-18; KuEx119* animals to adopt the double-mutant phenotype (Fig. 1A,B). As previously described, *lin-35* single mutants are viable but show a substantial reduction in brood sizes compared with wild type (Table 1) (Lu and Horvitz, 1998; Fay et al., 2002). Similarly, *ubc-18* single mutants exhibit a marked reduction in brood size and are slightly growth retarded (Table 1; data not shown).

Approximately 4% of *lin-35; ubc-18* larvae display a Pun (pharyngeal unattached) phenotype, whereby the pharynx has failed to elongate and form an attachment to the anterior alimentary opening or buccal cavity (Fig. 1C,D; Table 1). Such animals fail to ingest food and arrest growth during the first larval stage. The frequency of Pun animals was dramatically increased following inactivation of *lin-35* by RNAi in either a *lin-35; ubc-18; KuEx119* or *ubc-18* single-mutant background (Table 1; data not shown). This difference in the penetrance of the Pun phenotype between *lin-35; ubc-18* and *ubc-18; lin-35(RNAi)* animals may be due to a low frequency of LIN-35 maternal rescue derived from the extrachromosomal array. Alternatively, although less likely, *lin-35(n745)*, a strong loss-of-function allele containing an early nonsense mutation (Lu and Horvitz, 1998), may have some residual activity. The cause for growth arrest in *lin-35; ubc-18* animals that contain normal-appearing pharynges is currently unknown. It is possible that such animals are defective at feeding because of more subtle alterations in pharyngeal structure or attachments. However, as

Table 1. Viability of *lin-35* and *ubc-18* mutant derivatives

| | % Larval arrest* | % Pun | % Sterile | Average brood size |
|--|------------------|------------|------------------------|-------------------------------|
| N2 | <1 (many) | 0 (n=260) | <1 (many) | 264 (±18) (n=50) [†] |
| <i>lin-35</i> (n745) | 1 (n=268) | 0 (n=268) | 4 (n=100) [†] | 98 (±43) (n=10) [†] |
| <i>ubc-18</i> (<i>ku354</i>) | 3 (n=223) | 0 (n=101) | 3 (n=30) | 79 (±28) (n=14) |
| <i>lin-35; ubc-18</i> | 84 (n=192) | 4 (n=192) | 72 (n=30) | 3 (±2) (n=7) |
| <i>ubc-18; lin-35</i> (RNAi) | 87 (n=145) | 46 (n=171) | ND | ND |
| <i>lin-35; ubc-18/+^{mat-‡}</i> | 42 (n=185) | 2 (n=185) | 43 (n=30) | 45 (±46) (n=17) |
| <i>lin-35; ubc-18/+^{mat+§}</i> | 12 (n=245) | 0 (n=245) | 32 (n=28) | 54 (±39) (n=10) |
| <i>ubc-18/+[¶]</i> | 0 (n=121) | 0 (n=121) | 10 (n=20) | 271 (±42) (n=10) |
| <i>lin-35; ubc-18/ubc-18/+^{mat+**}</i> | ND | ND | 22 (n=50) | 58 (±32) (n=11) |
| N2 RNAi feeding control ^{††} | ND | ND | 0 (n=20) | 250 (±41) (n=8) |
| N2 <i>ubc-18</i> (RNAi) | 0 (n=100) | 0 (n=100) | 0 (n=30) | 221 (±23) (n=8) |
| <i>rrf-3</i> | 0 (n=100) | 0 (n=100) | 0 (n=20) | 72 (±37) (n=10) |
| <i>rrf-3; ubc-18</i> (RNAi) | 0 (n=103) | 0 (n=103) | 0 (n=20) | 36 (±14) (n=10) |
| <i>lin-35; ubc-18</i> (RNAi) | 5 (n=110) | 0 (n=255) | 23 (n=30) | 55 (±34) (n=10) |
| <i>lin-35; rrf-3</i> | 2 (n=102) | 0 (n=102) | 45 (n=42) | 52 (±33) (n=10) |
| <i>lin-35; rrf-3; ubc-18</i> (RNAi) | 21 (n=265) | 0 (n=265) | 100 (n=40) | ND |
| <i>lin-35; ubc-18</i> (<i>ku354</i>); <i>ubc-18</i> (RNAi) | 91 (n=140) | 40 (n=174) | 77 (n=30) | 2 (±2) (n=7) |

*Animals either died as larvae or failed to reach maturity after 5 days.

[†]Fay et al., 2002.

[‡]Heterozygous animals were obtained by mating *lin-35* males to *lin-35; dpy-17, ubc-18, unc-32; kuEx119* hermaphrodites and scoring effects in the non-DpyUnc *kuEx119*-progeny. Animals with the genotype *lin-35; dpy17, unc-32/+* were found to have brood sizes indistinguishable from that of *lin-35* animals [95 (±51) (n=10) versus 98 (±43)]. Mat-, maternally deficient for *ubc-18*.

[§]Males generated from the cross described above were in turn mated to *lin-35; unc-46, dpy-11* hermaphrodites, and non-DpyUnc cross progeny were scored for larval arrest. Because only half the expected progeny would be expected to contain the *dpy-17, ubc-18, unc-32* chromosome, the percentage of larval arrest was adjusted accordingly. Brood sizes were calculated from animals that threw both *dpy-17, ubc-18, unc-32* and *unc-46, dpy-11* progeny. Mat+, maternally wild type for *ubc-18*.

[¶]Heterozygous animals were generated by mating N2 males to *unc-32, ubc-18* hermaphrodites.

**The free duplication *qDp3* was used for these analyses. For further details, see Materials and Methods.

^{††}The empty vector pPD129.36 was used as a control for all RNAi feeding experiments.

most of these animals do undergo some degree of growth prior to arrest, their defect may be unrelated to their ability to feed. No obvious abnormalities in the proliferation or differentiation of other somatic cells were observed in *lin-35; ubc-18* double mutants that reach adulthood (data not shown).

We also observed a high incidence of larval arrest in animals that were homozygous for *lin-35*, but heterozygous for *ubc-18*, though the rate of arrest was lower than that observed for homozygous double mutants (Table 1). In addition, *lin-35; ubc-18/+* animals that reached adulthood showed an ~50% reduction in brood size compared with *lin-35* mutants alone (Table 1). These results suggest that the *ubc-18* mutation could be semi-dominant or haplo-insufficient, or, based on the method used to generate the heterozygous animals, *ubc-18* could be maternally required. Further experiments indicated that the effect in heterozygous animals results from a combination of the latter two possibilities: (1) *lin-35* mutant animals that are heterozygous, but maternally wild type, for *ubc-18* show lower rates of larval arrest than those that are heterozygous but maternally deficient (Table 1); thus, the presence of maternal *ubc-18* can partially reduce the severity of *lin-35; ubc-18* genetic interactions; (2) overexpression of the *ku354* variant of UBC-18 (via an extrachromosomal array), together with *lin-35* inactivation by RNAi, did not lead to a phenocopy of the double-mutant phenotype (data not shown); (3) in an otherwise wild-type background, *ubc-18/+* heterozygous animals had wild-type brood sizes, indicating that the effects in heterozygous animals were specific to *ubc-18* genetic interactions with *lin-35* (Table 1); and (4) RNAi of *ubc-18* performed on *lin-35; ubc-18; kuEx119* animals

strongly enhanced the penetrance of the Pun phenotype in progeny not harboring the array compared with the array-deficient progeny of untreated *lin-35; ubc-18; kuEx119* animals [Table 1 and see discussion of *ubc-18*(RNAi) below]. This latter result also indicates that *ku354* represents a partial loss-of-function allele of *ubc-18*.

We also carried out further genetic analysis using a regional free duplication (*qDp3*) that contains sequences from an ~0.5 Mb region of chromosome III, including *ubc-18*. Briefly, we found that *lin-35; ubc-18/ubc-18; qDp3* animals displayed a similar phenotype to *lin-35; ubc-18/+* animals (Table 1 and data not shown), further supporting our conclusion that *ku354* is a LOF allele and does not act in a dominant or dose-dependent manner. We note that we were unable to generate stable strains that were heterozygous for *ubc-18* and *nDf16* (a large chromosomal deficiency that deletes *ubc-18*) in the *lin-35; KuEx119* background, as the *lin-35* mutation surprisingly showed a synthetic genetic interaction with the deficiency itself (also see Materials and Methods).

***ubc-18* encodes a homolog of the ubiquitin activating enzyme UbCH7**

ku354 was mapped to a small segment of chromosome III between *sma-3* and *unc-32* using genetic markers and single-nucleotide polymorphisms (SNPs). To identify the affected gene, *lin-35; ubc-18; KuEx119* animals were co-injected with regional cosmids and a dominant marker conferring a Rol phenotype. Rescued lines were identified by the presence of healthy Rol animals that no longer required the original array containing *lin-35* (*kuEx119*) for viability. Two overlapping

| | | | |
|--------|--|---------|-----|
| | | *(E10K) | |
| UBC-18 | MSATRRLQKELGDLKNCGVKAYENVECEETNLLKWTVLLIPDKEPYNKCAFK | | 52 |
| UBCH7 | MAASRRRLMKELLEIRKCGMKNFERNIQVDEANLLTWQGLVLPDNPYDKCAFK | | 52 |
| Ubc5 | MSSSRRIAKELSDLGRDPPFASCAGPVGDDLHYHQASIMCPDSDSPVAGCVFF | | 52 |
| | | | |
| UBC-18 | VCITFPVDYPPFKPPKVAEETKTYHPNVDEEGKFCLEPVTAEENWKPAKTEOV | | 104 |
| UBCH7 | IEINFPFAEYPPFKPPKLTETKTYHPNIDEKGOVCLPVI SAENWKPAKTEOV | | 104 |
| Ubc5 | LSLHFFFDYPPFKPPKVNETKTYHPNINSSGNICLEDILKDO--WSPALTLKSV | | 103 |
| | | | |
| UBC-18 | MMALLSTINEPEPSEHETRADVAEEFQDHHKFMKTAEBHTRKHAEKRP-E | | 153 |
| UBCH7 | IQSLIALVNDPQPEHPLRADLAEYSKDRKPKCKNABEFTKRYGKRPVD | | 154 |
| Ubc5 | LLSICSLTLDANPDELVEPAQIYKTDKAKYEATAKRWTKQYAV---- | | 148 |

Fig. 2. Alignment of UBC-18 with UBCH7 and Ubc5. Clustal analysis was used to align *C. elegans* UBC-18 with UBCH7 from humans and Ubc5 from *S. cerevisiae*. Black boxes indicate identity; gray boxes indicate similarity. The location of the mutation in *ku354* mutant animals is indicated by an asterisk.

cosmids in the region, R01H2 and C49B6, were found to rescue the *lin-35; ubc-18* synthetic lethality. A minimal rescuing sequence was identified that contained only a single predicted open reading frame: that encoding the *C. elegans* gene *ubc-18/R01H2.6*. Six out of eight independently derived transgenic lines containing the wild-type *ubc-18* gene efficiently rescued the double-mutant phenotype (also see Materials and Methods).

ubc-18 encodes a predicted protein of 153 amino acids that is highly similar to known E2-type ubiquitin-conjugating enzymes (Jones et al., 2002). UBC-18 shows greatest similarity to UbcH7 in humans (29% identical and 86% similar) and is approximately equally similar to *S. cerevisiae* proteins Ubc-5p and Ubc-4p (Fig. 2; data not shown). The database prediction for *ubc-18* is supported by the existence of multiple sequenced cDNA clones (kindly provided by Y. Kohara) that confirm both the 3' terminus of the gene as well as the precise locations of its four exons. In addition, the 5' untranslated region that was identified by the cDNA clones contains two in-frame stop codons located just upstream (15 and 24 nucleotides) of the start ATG.

We sequenced the entire genomic region of *ubc-18* from *ku354* mutant animals and identified a single lesion that resulted in a nonconservative amino acid substitution at position 10 of UBC-18. The mutation converts a glutamic acid residue that is highly conserved in many E2 proteins to a lysine (Fig. 2 and data not shown). This region of the protein facilitates interactions of E2 enzymes with E1 ubiquitin-activating enzymes (Haas and Siepmann, 1997; Tong et al., 1997) and may play a minor role in interactions with some E3 ubiquitin ligases (Huang et al., 1999; Zheng et al., 2000; Martinez-Noel et al., 2001). A failure to interact with E1 (or with E3) enzymes would be predicted to result in a strong loss of function in this E2, or could possibly lead to an E2 with dominant-negative activity (Townsend et al., 1997; Yamanaka et al., 2000) (however, see previous discussion concerning haploinsufficiency).

RNAi of *ubc-18* has previously been reported to have no phenotype in wild-type animals (Jones et al., 2002). Consistent with this, we observed, at most, a subtle effect of *ubc-18(RNAi)* on viability and brood size in N2 animals, although treated animals generally took an extra day to reach maturity when compared with control animals (Table 1; data not shown). Mutations in *rrf-3*, a predicted RNA-directed RNA polymerase, have recently been reported to enhance the overall efficacy of gene inactivation by RNAi feeding methods (Simmer et al., 2002). Consistent with this, RNAi inactivation of *ubc-18* in the *rrf-3* mutant background led to an ~50%

reduction in brood size when compared with *rrf-3* mutants alone (Table 1).

To see if we could reiterate the double-mutant phenotype, we performed *ubc-18(RNAi)* on *lin-35* and *lin-35; rrf-3* animals. RNAi treatment of *lin-35; rrf-3* double mutants resulted in first-generation progeny that either arrested as larvae or developed into completely sterile adults (Table 1). These adults often failed to generate sperm and contained abnormal-appearing oocytes, similar to some *lin-35; ubc-18* double mutants (data not shown). We note that even without RNAi treatment, *lin-35; rrf-3* double mutants were markedly less healthy than either *lin-35* or *rrf-3* single mutants (Table 1). Treatment of *lin-35* mutants with *ubc-18(RNAi)* led to more subtle defects in the first generation (Table 1), though prolonged exposure resulted in higher rates of larval arrest and adult sterility in subsequent generations (data not shown).

We failed to observe any Pun animals arising from *ubc-18(RNAi)* treatment of *lin-35* or *lin-35; rrf-3* animals (Table 1) or in experiments where both genes were simultaneously inactivated by RNAi (data not shown). Such results may reflect a failure to sufficiently inactivate *ubc-18* by RNAi methods, or they may occur if strong inactivation of *ubc-18* led to sterility of the treated parent prior to the production of Pun progeny.

lin-35; ubc-18 embryos are defective at pharyngeal morphogenesis

An initial examination of both *lin-35; ubc-18* and *ubc-18; lin-35(RNAi)* embryos (hereafter referred to as double-mutant embryos) indicated that the first observed defects in pharyngeal development coincided with events taking place at or just prior to the 1.5-fold stage of embryogenesis. At this time in wild-type animals, a subset of anterior pharyngeal cells reorient their longitudinal axes, form associations with neighboring cells and then shift their positions towards the anterior region of the embryo through a localized contraction mechanism, leading to pharyngeal elongation (Portereiko and Mango, 2001) (see below). By contrast, pharyngeal cells of double-mutant embryos remain stationary and fail to move towards the anterior (Fig. 3A-D). In addition, whereas the anterior border of the basement membrane that encapsulates the pharyngeal primordium becomes less distinct during elongation in wild-type embryos, this feature remains prominent in the double mutants (Fig. 3A,C; see Fig. 5). The failure of mutant embryos to undergo pharyngeal elongation could result from several distinct underlying defects: (1) mutant embryos may generate incorrect numbers of pharyngeal precursor cells during early embryonic development, leading to defects at later stages; (2) these precursor cells, once generated, may fail to differentiate

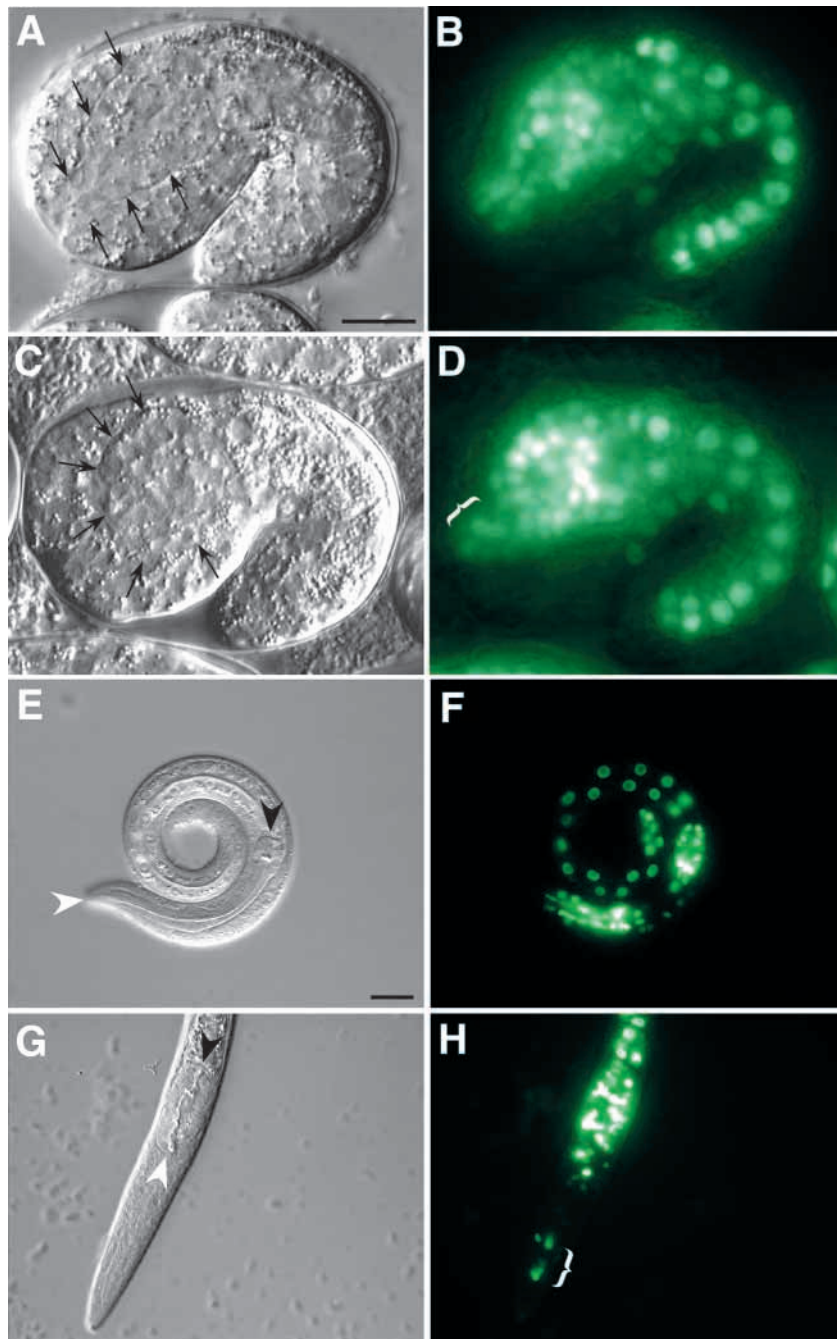


Fig. 3. *pha-4::GFP* expression in wild-type and mutant animals. DIC (A,C,E,G) and corresponding *pha-4::GFP* fluorescence (B,D,F,H) images. (A-D) ~1.5-fold-stage wild-type (A,B) and *ubc-18; lin-35(RNAi)* mutant (C,D) embryos. Anterior is towards the left and ventral is downwards. Arrows indicate the dorsoventral pharyngeal boundaries. Note gross differences in pharyngeal shape and borders in double mutants versus wild-type embryos. In addition, note the overall similarity in the numbers of GFP-expressing cells in wild-type and double-mutant embryos. (The mutant and wild-type embryos contained 102 and 101 GFP+ nuclei, respectively.) The white bracket (D) demarcates the presence of several GFP-expressing arcade cells that failed to integrate with the rest of the pharynx. Intestinal cell nuclei, which are large, round and reside to the posterior, can readily be distinguished from pharyngeal nuclei at this stage. (E-H) *pha-4::GFP* expression in wild-type (E,F) and *ubc-18; lin-35(RNAi)* mutant L1 larvae (G,H). White and black arrowheads indicate anterior and posterior pharyngeal boundaries, respectively. As above, note the overall similarity in the number of GFP-expressing cells in contrast to the gross differences in pharyngeal shape between wild-type and double-mutant animals. The bracket (H) indicates the non-integrated arcade cells. Scale bars: in A, 10 μ m for A-D; in E, 10 μ m for E-H.

embryos. In addition, the relative distribution of most pharyngeal nuclei did not vary significantly between Pun and wild-type embryos at this time, allowing for an even comparison.

An examination of wild-type embryos at the 1.5-fold stage identified an average of 100 ± 3 ($n=11$; range, 95–104) GFP+ cells in the head region. This figure is in close agreement with previously reported numbers using antibodies against PHA-4 in similar-stage embryos (97 ± 3) (Horner et al., 1998) (Fig. 3A,B). An analysis of Pun double-mutant embryos revealed an average of 93 ± 13 GFP+ cells ($n=13$) with numbers ranging from 66–105. Importantly, 8/13 mutant embryos contained 95 or more GFP+ cells, whereas only 3/13 contained fewer than 91 cells (Fig. 3C,D). Thus, for most embryos examined, the number of cells adopting a pharyngeal identity (based on this GFP marker) was

properly; and (3) properly specified pharyngeal cells may fail to execute one or more steps during morphogenesis of the organ.

To test this first possibility we assayed the number of pharyngeal cells in mutant embryos using a GFP reporter, *pha-4::GFP* (kindly provided by S. Mango), which is strongly expressed in the nuclei of both primordial and differentiated pharyngeal cells as well as in cells comprising the posterior intestinal tract (Horner et al., 1998). We focused on embryos at the 1.5-fold stage, as this period of development coincided with the first observed defects in our double mutants. Importantly, at this stage, mutant embryos that had failed to initiate elongation could be readily distinguished from wild-type-appearing

indistinguishable from that of wild type. Similar results were also obtained by examining *pha-4::GFP*-expressing cells in L1 larvae of double-mutant and wild-type animals (Fig. 3E-H; data not shown). These findings indicate that gross differences in the number of pharyngeal cells alone cannot account for the observed defects in a large subset (perhaps the majority) of the double-mutant embryos. Thus, the failure to elongate is probably unrelated to early steps of pharyngeal cell specification or survival.

We next examined mutant animals for their ability to generate terminally differentiated pharyngeal cell types. The adult pharynx comprises muscle, epithelial and neuronal cells, as well as marginal and gland cell types (Albertson and

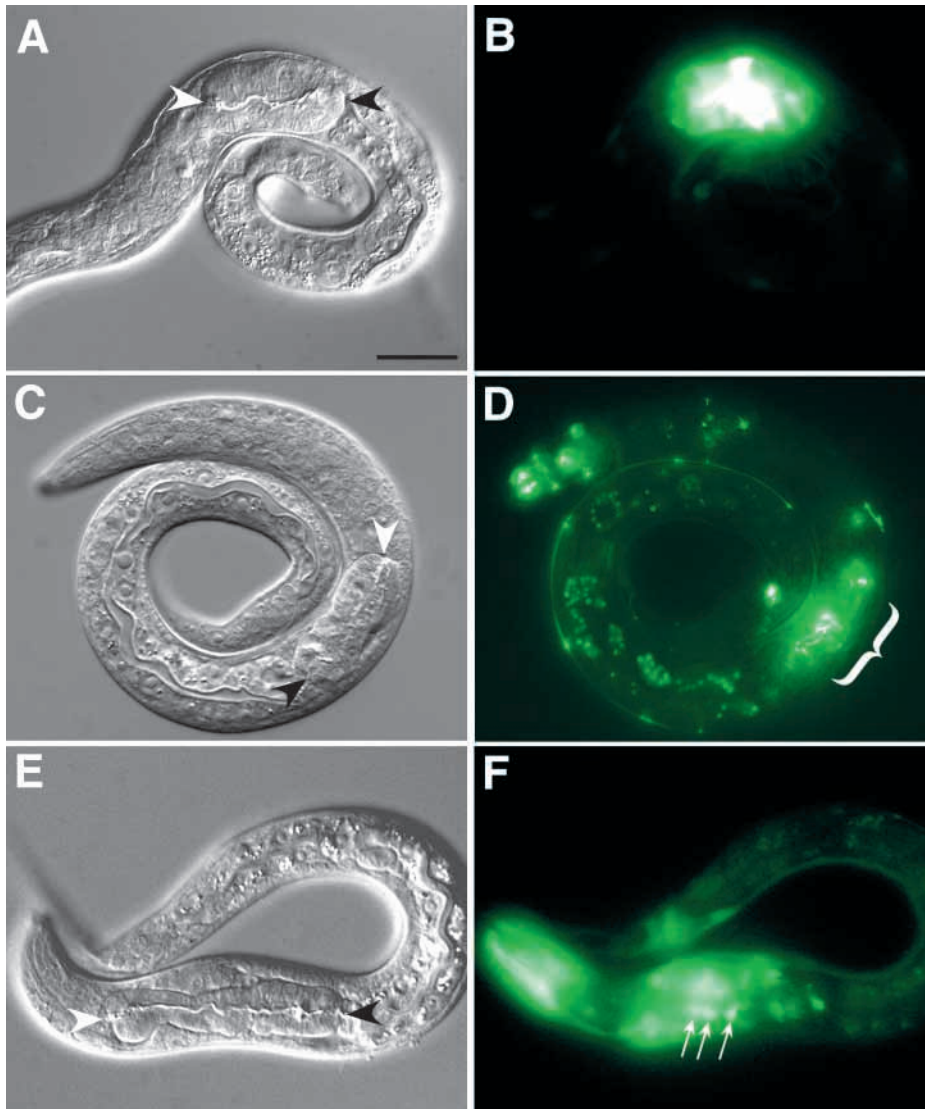


Fig. 4. Expression of differentiation markers in mutant animals. DIC (A,C,E) and corresponding GFP fluorescence (B,D,F) images of *ubc-18; lin-35(RNAi)* mutant animals. White and black arrowheads indicate anterior and posterior pharyngeal boundaries, respectively. (A,B) Expression of the differentiated muscle cell marker, *myo-2::GFP*. (C,D) Expression of the adherens junction component and marker for epithelial cell differentiation, *ajm-1::GFP*. Bracket indicates the region of *ajm-1* expression in the non-extended pharynx. (E,F) Neuronal marker (*unc-119::GFP*) expression in a pharynx that underwent partial extension. White arrows (F) indicate the positions of several GFP+ nuclei that lie within the pharyngeal borders. Scale bar: 10 μ m.

at which elongation may fail. Morphogenesis of the pharynx can be formally divided into three distinct steps, all of which occur over a relatively short time frame, beginning at the late comma stage of embryonic development, or \sim 330 minutes into embryonic development (Porteriko and Mango, 2001) (Fig. 5M). During stage I of morphogenesis, epithelial cells in the anterior region of the pharyngeal primordium reorient their long axes to align with the dorsoventral axis of the embryo. At stage II, arcade cells, which reside between the pharyngeal primordium and the buccal cavity, form a continuous epithelium with the newly reoriented pharyngeal epithelial cells. At stage III, the conjoined arcade and anterior pharyngeal cells undergo a

contraction, pulling the pharynx towards the buccal cavity.

To aid in our analysis, we used a reporter strain that expresses a membrane-localized GFP-fusion protein under the control of the *pha-4* promoter (kindly provided by S. Mango), which allowed us to follow changes in pharyngeal cell shape. In wild-type embryos, elongation was completed by the 1.5-fold stage of embryonic development (\sim 400 minutes into embryonic development; Fig. 5A-D). By contrast, 17 of the 24 double-mutant embryos displayed clear defects in the ability of anterior epithelial cells to initiate or complete the reorientation step (Stage I; Fig. 5E-L). Interestingly, a substantial fraction of the orientation-defective embryos (9/17) were only partially deficient at this step, such that one or more epithelial cells appeared to correctly shift their axes, whereas others remained in their original orientation (Fig. 5I-L). Other mutant embryos (7/24) exhibited more complex and variable defects such as a general disorganization of the leading-edge cells (data not shown). Taken together, these results indicate that *lin-35* and *ubc-18* functionally cooperate to control a crucial and early step of pharyngeal morphogenesis during *C. elegans* development.

Thomson, 1976; Sulston and Horvitz, 1977). We used several different GFP reporter strains to assay for the presence of muscle (Okkema et al., 1993), epithelial (Mohler et al., 1998) and neuronal cells (Maduro and Pilgrim, 1995) in double-mutant embryos and larvae. We found that all three cell types were produced, indicating that mutants are capable of generating most or all of the correct pharyngeal cell types (Fig. 4). Consistent with this, we have observed sustained rhythmic pumping in many severely Pun pharynges of L1 mutant animals, suggesting that most or all terminal cell types have been specified and are physiologically functional, although the overall pharyngeal structure is grossly perturbed. We note that our level of analysis does not allow us to make conclusions regarding the differentiation status of individual cells within the pharynx. Therefore, it is possible that double mutants may contain a subset of improperly or incompletely differentiated pharyngeal cells that could contribute to the observed defects.

Given that many of the affected double mutants generate normal numbers of pharyngeal cells that are capable of differentiation, we decided to look closely at early steps of pharyngeal morphogenesis to determine the precise point

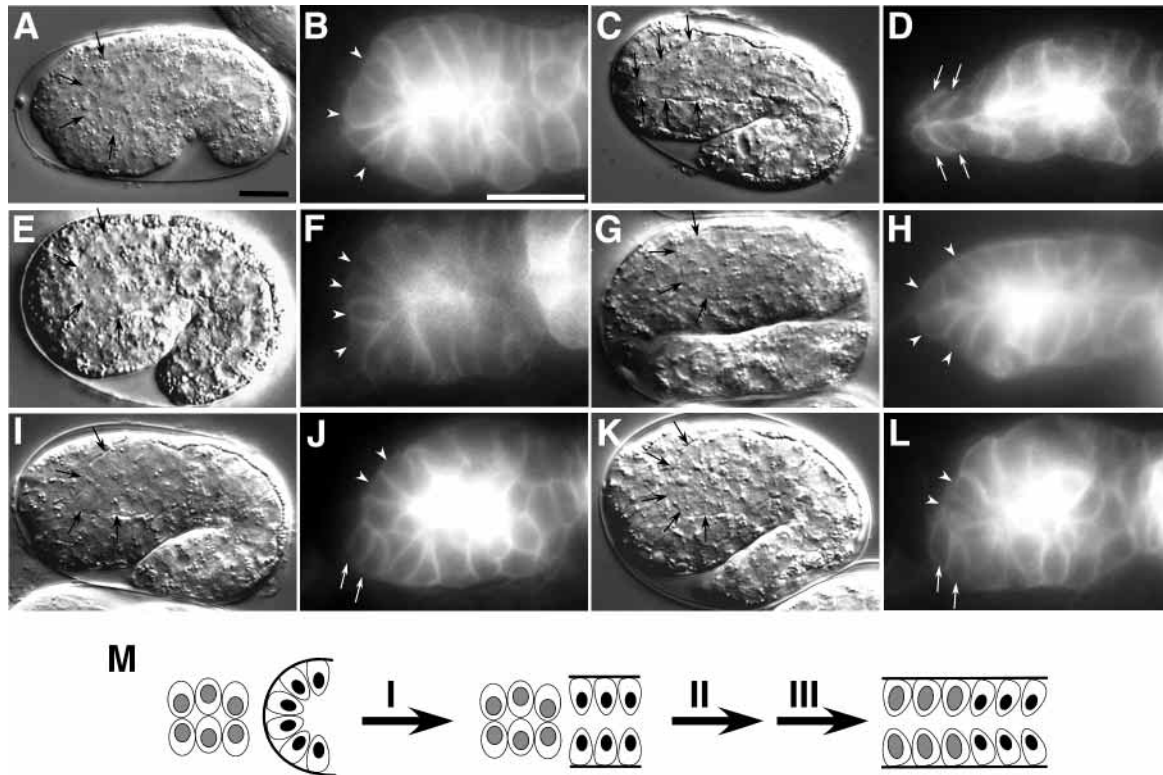


Fig. 5. Pharyngeal morphogenesis in wild-type and mutant animals. DIC (A,C,E,G,I,K) and corresponding GFP fluorescence (B,D,F,H,J,L) images showing the outline of pharyngeal (and intestinal) cells in wild-type (A-D) and *ubc-18; lin-35(RNAi)* mutant (E-L) embryos. Anterior is towards the left and ventral is downwards. Black arrows demarcate the anterior pharyngeal boundary. (M) A schematic for pharyngeal extension involving three discrete steps (also see text). (A,B) An early comma-stage embryo, before overt signs of morphogenesis have begun. Note the teardrop shape of the leading-edge epithelial cells (white arrowheads, B). (C,D) 1.5-fold-stage embryo with pharynx now extended to the anterior. Note the transformation in the shape of the leading-edge epithelial cells (white arrows, D). (E,F) 1.5-fold and (G,H) 2-fold-stage mutant embryos where leading edge epithelial cells have failed to reorient (white arrowheads in F,H). (I-L) 1.5-fold-stage mutant embryos in which dorsal epithelial cells have failed to reorient their axes (white arrowheads) whereas ventral cells in the same embryo appear to have undergone the proper transformation (white arrows). (M) Pharyngeal extension with three distinct steps (Portereiko and Mango, 2001) (see text). Scale bars: in A, 10 μ m for A,C,E,G,I,K; in B, 10 μ m for B,D,F,H,J,L.

ubc-18 interactions with SynMuv genes

Previous studies on *fzr-1/slr-1* demonstrated a limited set of genetic interactions with class B synthetic multivulval (SynMuv) gene family members (Fay et al., 2002). To determine the spectrum of *ubc-18* genetic interactions, we inactivated class B SynMuv genes in *ubc-18* mutants by RNAi feeding methods and assayed progeny for the appearance of the Pun phenotype (Table 2). All but one of the class B genes tested produced substantial numbers of Pun animals following inactivation by RNAi. These included *lin-36* (Thomas and Horvitz, 1999) and *lin-37* (Boxem and van den Heuvel, 2002), two genes of unknown function; the RbAp46/48 homolog, *lin-53* (Lu and Horvitz, 1998); a *C. elegans* Mi2 homolog and NURD complex component, *let-418* (Solari and Ahringer, 2000; von Zelewsky et al., 2000); and histone deacetylase, *hda-1* (Lu and Horvitz, 1998). The sole exception in the class B category was *efl-1*, one of two E2F homologs in *C. elegans* (Ceol and Horvitz, 2001), which failed to produce significant numbers of Pun animals either alone (data not shown) or in the *ubc-18* mutant background (Table 2). In addition, we saw no effect following inactivation of the class A SynMuv gene *lin-15a* (Clark et al., 1994; Huang et al., 1994). In several cases,

these experiments were complicated by non-synthetic RNAi effects as the genes that were being inactivated were themselves essential for viability (Table 2). Nevertheless, in such cases we were still able to observe a marked enrichment in the number of animals displaying the Pun phenotype, demonstrating that inactivation of these genes is interchangeable with *lin-35* for the production of this phenotype.

Recently, Boxem and van den Heuvel (Boxem and van den Heuvel, 2002) have shown an involvement of several SynMuv genes, including *lin-35*, *lin-36*, *efl-1* and *lin-15a*, in the regulation of the G1- to S-phase transition (also see Boxem and van den Heuvel, 2001). Consistent with this, we had previously observed genetic interactions between *fzr-1* and *lin-35*, *lin-36* and *efl-1* in the production of a synthetic hyperproliferation phenotype (Fay et al., 2002). By contrast, *lin-37*, *let-418*, *lin* and *hda-1* did not appear to function in cell cycle control (Boxem and van den Heuvel, 2002). Thus, the ability of these genes to interact with *ubc-18* suggests that the synthetic Pun phenotype does not result from perturbations in cell cycle control per se, and that the role of *lin-35* in pharyngeal development is probably not related to its role in regulating cell cycle progression.

Table 2. Genetic interactions of *ubc-18* with SynMuv genes

| | Percentage Pun* |
|---|-------------------------|
| N2 (wild type) | 0 (many) |
| <i>ubc-18</i> | 0 (n=101) |
| <i>lin-35</i> (RNAi) | 0 (n=50) |
| <i>ubc-18; lin-35</i> (RNAi) | 46 (n=171) |
| <i>lin-36</i> (RNAi) | 0 (n=58) |
| <i>ubc-18; lin-36</i> (RNAi) | 36 (n=52) |
| <i>lin-37</i> (RNAi) | 0 (n=62) |
| <i>ubc-18; lin-37</i> (RNAi) | 14 (n=132) |
| <i>lin-53</i> (RNAi) [†] | 0 (n=73) |
| <i>ubc-18; lin-53</i> (RNAi) [†] | 36 (n=126) |
| <i>let-418/chd-4</i> (RNAi) [†] | 1 (n=313) |
| <i>ubc-18; let-418</i> (RNAi) | 14 (n=93) |
| <i>hda-1</i> (RNAi) [†] | 1 (n=60) |
| <i>ubc-18; hda-1</i> (RNAi) | 6 (n=94) |
| <i>ubc-18; eft-1</i> (RNAi) [‡] | <1 (n=245) [‡] |
| <i>ubc-18; lin-15a</i> (RNAi) | 0 (n=50) |

*Includes both non- and partially elongated pharynges.

[†]RNAi of these genes caused low to moderate levels of sterility and embryonic lethality.

[‡]One out of 245 larvae examined showed a Pun phenotype.

DISCUSSION

Isolation of a mutation in an E2 ubiquitin-conjugating enzyme

Using a screen for mutations that are synthetically lethal with pRB, we have identified a mutation in *ubc-18*, a gene encoding a putative E2 ubiquitin-conjugating enzyme. The nature of the molecular lesion identified in *ubc-18* (*ku354*) mutants, as well as our RNAi analysis, suggests that *ku354* may represent a strong loss-of-function allele. The alteration in chemical charge resulting from the E10K mutation occurs in a region that is required for association with E1 activating enzymes (Haas and Siepmann, 1997; Tong et al., 1997). Several conserved basic residues in this region (equivalent to amino acids R5, R6, and K9 in UBC-18) have been identified as biochemically important for interactions with E1 enzymes (A. Haas, personal communication). Furthermore, the glutamic acid at position ten is highly conserved among many UBCs, including those of the UbcH7 family (Fig. 2; data not shown). Thus, it is likely that the E10K mutation would greatly reduce or abolish interactions between UBC-18 and the upstream E1 activating enzyme, preventing the conjugation of UBC-18 to ubiquitin.

A recent global analysis of gene expression using microarrays in *C. elegans* indicates that the *ubc-18* transcript is present at significant levels in both oocytes and embryos, as well as in late stages of larval development and into adulthood (Hill et al., 2000). In addition, using antibodies, LIN-35 has been shown to be expressed throughout development in most or all cell types (Lu and Horvitz, 1998). We were unsuccessful in our attempts to generate transgenic animals that express GFP under the control of the *ubc-18* promoter using several different reporter constructs (data not shown). Given that transgenic arrays are typically silenced in the *C. elegans* germline, our results may indicate that *ubc-18* expression is germline specific. Consistent with this, data available on the *C. elegans* expression database (<http://nematode.lab.nig.ac.jp/db/>

index.html; kindly provided by Y. Kohara) suggest that *ubc-18* expression may be largely or completely restricted to germline cells. Germline expression of UBC-18 is also consistent with our observation that maternal *ubc-18* function markedly reduced larval lethality in *lin-35; ubc-18/+* animals (Table 1).

A genetic interaction between *lin-35*/Rb and a ubiquitin pathway component

ubc-18 is the second gene that we have identified as a *lin-35*-synthetic mutation. Simultaneous inactivation of *lin-35* and *ubc-18* led to growth arrest, infertility and defects in pharyngeal morphogenesis. Based on known roles of these proteins, we believe that LIN-35 and UBC-18 share a set of common targets for transcriptional repression and ubiquitin-mediated degradation, respectively. We hypothesize that the abnormal expression of one or more mutual targets is probably responsible for the pleiotropic defects observed in the double mutants. Thus, in the absence of LIN-35 function, UBC-18 can promote the degradation of some subset of derepressed LIN-35 transcriptional targets. Conversely, UBC-18 function is not essential if LIN-35 is present and actively repressing the expression of its target genes. It is only when both *lin-35* and *ubc-18* are absent, that one or more proteins can accumulate to levels sufficient to produce the observed developmental defects.

It is also conceivable that the phenotype observed in the double mutants may not be due solely to defects resulting from an increase in the abundance of target proteins. It has become clear in recent years that ubiquitylation can affect protein function by mechanisms unrelated to protein stability. These functions include roles in protein trafficking (reviewed by Pickart, 2001), transcription (reviewed by Conaway et al., 2002) and signal transduction (Wang et al., 2001; Ulrich, 2003). Nevertheless, we currently favor a model whereby *lin-35* and *ubc-18* act coordinately to downregulate the activity of proteins whose presence would be deleterious to specific developmental processes or basic life functions.

Our analysis of the double-mutant animals identified a predominant defect affecting stage I of pharyngeal morphogenesis. This phenotype differs substantially from defects reported for two previously described pharyngeal mutants in *C. elegans*: *pha-1* and *pha-4*. *pha-4* mutants fail to specify any pharyngeal cells, which instead adopt alternative cell fates (Mango et al., 1994). In the case of *pha-1* mutants, the correct number of pharyngeal cells are initially specified; however, these cells then fail to undergo terminal differentiation (Schnabel and Schnabel, 1990; Granato et al., 1994). *pha-4* and *pha-1* encode transcription factors of the FoxA/HNF3 and bZIP families, respectively. *pha-4* directly activates the transcription of most or all genes required for pharyngeal identity (Gaudet and Mango, 2002). It is possible that *lin-35* and *ubc-18* act to downregulate one of the early *pha-4* target genes in order for morphogenesis to proceed. Alternatively, *lin-35* and *ubc-18* may negatively regulate genes that are not normally expressed in this tissue but whose expression is deleterious to the development of the organ.

A novel role for *lin-35*/Rb in morphogenesis and development

At present, relatively little is known about the targets of

pRb (particularly those unrelated to cell cycle progression) and even less is known about the substrates of most E2 and E3 enzymes. Given the genetic interactions that we observed between *ubc-18* and a number of the SynMuv genes tested (Table 2), it is unlikely that the targets of pRB that are involved in pharyngeal development also function in cell cycle control. Interestingly, we have isolated a second mutation, *slr-9(fdl)*, that produces a synthetic Pun phenotype in conjunction with *lin-35*. *slr-9* has been mapped to a small interval on LGIII that does not contain any predicted proteins with a known involvement in the protein degradation pathway (E.L. and D.S.F., unpublished). Thus, we may be poised to identify either novel components involved in ubiquitin pathway targeting or, possibly, specific effectors of pharyngeal development.

Extensive studies have defined a central and clear role for pRb in regulating entry and progression through the S-phase of the cell cycle. Genetic studies carried out in *Drosophila* have further suggested that pRb may act exclusively through E2F, as LOF mutations in *e2f1*, one of two *Drosophila* E2F homologs, can largely suppress the lethal phenotype of mutations in *rbf*, one of two known *Drosophila* Rb-family genes (Du, 2000). A separate role for pRb in differentiation, which is independent of its interactions with E2F, is, however, suggested by the observation that certain pRb mutants that are defective at E2F binding can nevertheless induce tissue-specific gene expression and promote differentiation (Sellers et al., 1998). In addition, using a cell line that overexpresses a non-regulatable form of pRb, Markey and colleagues (Markey et al., 2002) recently identified a large set of putative pRb transcriptional targets that are not known or predicted to be regulated by E2F family members. Finally, E2F family members themselves have been shown through microarray experiments to control the expression of a diverse set of targets including a number of genes associated with differentiation and development (Ishida et al., 2001; Muller et al., 2001).

Thus, our synthetic lethal screen has uncovered a function for *lin-35/Rb* that is distinct from those previously described for pRB in higher eukaryotes. Additional developmental functions of *lin-35* should be revealed by the further analysis of *lin-35* synthetic mutants and by looking directly for interactions between *lin-35* and other putative E2 and E3 enzymes using an RNAi approach. Furthermore, by identifying specific phenotypes for putative E2 and E3 enzymes, it may also be possible to make predictions regarding the functional and biochemical associations between the many E2 and E3 enzymes present in the *C. elegans* genome.

We thank the *C. elegans* Genetics Consortium, Susan Mango, Jeff Hardin, Peter Candido, Andy Fire and David Pilgrim for strains and constructs. We thank Alan Coulson for cosmids. We also thank Susan Mango, Peter Candido, Eric Lambie and Arthur Hass for helpful discussions. We thank Yuji Kohara for his expression and EST database. We thank Amy Fluet, Mike Krause and John Yochem for a critical reading of this manuscript. This work was supported by a research grant from the American Cancer Society, the University of Wyoming, and by NIH grant GM47869.

REFERENCES

- Albertson, D. G. and Thomson, J. N. (1976). The pharynx of *Caenorhabditis elegans*. *Philos. Trans. R. Soc. Lond. B Biol. Sci.* **275**, 299-325.
- Boxem, M. and van den Heuvel, S. (2001). *lin-35* Rb and *cki-1* Cip/Kip cooperate in developmental regulation of G1 progression in *C. elegans*. *Development* **128**, 4349-4359.
- Boxem, M. and van den Heuvel, S. (2002). *C. elegans* class B synthetic multivulva genes act in G(1) regulation. *Curr. Biol.* **12**, 906-911.
- Brehm, A., Miska, E. A., McCance, D. J., Reid, J. L., Bannister, A. J. and Kouzarides, T. (1998). Retinoblastoma protein recruits histone deacetylase to repress transcription. *Nature* **391**, 597-601.
- Ceol, C. J. and Horvitz, H. R. (2001). *dpl-1* DP and *eft-1* E2F act with *lin-35* Rb to antagonize Ras signaling in *C. elegans* vulval development. *Mol. Cell* **7**, 461-473.
- Chen, P. L., Riley, D. J., Chen, Y. and Lee, W. H. (1996a). Retinoblastoma protein positively regulates terminal adipocyte differentiation through direct interaction with C/EBPs. *Genes Dev.* **10**, 2794-2804.
- Chen, P. L., Riley, D. J., Chen-Kiang, S. and Lee, W. H. (1996b). Retinoblastoma protein directly interacts with and activates the transcription factor NF-IL6. *Proc. Natl. Acad. Sci. USA* **93**, 465-469.
- Clark, S. G., Lu, X. and Horvitz, H. R. (1994). The *Caenorhabditis elegans* locus *lin-15*, a negative regulator of a tyrosine kinase signaling pathway, encodes two different proteins. *Genetics* **137**, 987-997.
- Conaway, R. C., Brower, C. S. and Conaway, J. W. (2002). Emerging roles of ubiquitin in transcription regulation. *Science* **296**, 1254-1258.
- DeGregori, J., Kowalik, T. and Nevins, J. R. (1995). Cellular targets for activation by the E2F1 transcription factor include DNA synthesis- and G1/S-regulatory genes. *Mol. Cell. Biol.* **15**, 4215-4224.
- DeGregori, J., Leone, G., Miron, A., Jakoi, L. and Nevins, J. R. (1997). Distinct roles for E2F proteins in cell growth control and apoptosis. *Proc. Natl. Acad. Sci. USA* **94**, 7245-7250.
- Dou, Q. P., Zhao, S., Levin, A. H., Wang, J., Helin, K. and Pardee, A. B. (1994). G1/S-regulated E2F-containing protein complexes bind to the mouse thymidine kinase gene promoter. *J. Biol. Chem.* **269**, 1306-1313.
- Du, W. (2000). Suppression of the *rbf* null mutants by a *de2f1* allele that lacks transactivation domain. *Development* **127**, 367-379.
- Dunaief, J. L., Strober, B. E., Guha, S., Khavari, P. A., Alin, K., Luban, J., Begemann, M., Crabtree, G. R. and Goff, S. P. (1994). The retinoblastoma protein and BRG1 form a complex and cooperate to induce cell cycle arrest. *Cell* **79**, 119-130.
- Duronio, R. J. and O'Farrell, P. H. (1995). Developmental control of the G1 to S transition in *Drosophila*: cyclin E is a limiting downstream target of E2F. *Genes Dev.* **9**, 1456-1468.
- Dyson, N. (1998). The regulation of E2F by pRB-family proteins. *Genes Dev.* **12**, 2245-2262.
- Eberhard, D. and Busslinger, M. (1999). The partial homeodomain of the transcription factor Pax-5 (BSAP) is an interaction motif for the retinoblastoma and TATA-binding proteins. *Cancer Res.* **59**, S1716-S1725.
- Fay, D. S., Keenan, S. and Han, M. (2002). *fzr-1* and *lin-35/Rb* function redundantly to control cell proliferation in *C. elegans* as revealed by a nonbiased synthetic screen. *Genes Dev.* **16**, 503-517.
- Fire, A., Xu, S., Montgomery, M. K., Kostas, S. A., Driver, S. E. and Mello, C. C. (1998). Potent and specific genetic interference by double-stranded RNA in *Caenorhabditis elegans*. *Nature* **391**, 806-811.
- Fraser, A. G., Kamath, R. S., Zipperlen, P., Martinez-Campos, M., Sohrmann, M. and Ahringer, J. (2000). Functional genomic analysis of *C. elegans* chromosome I by systematic RNA interference. *Nature* **408**, 325-330.
- Gaudet, J. and Mango, S. E. (2002). Regulation of organogenesis by the *Caenorhabditis elegans* FoxA protein PHA-4. *Science* **295**, 821-825.
- Granato, M., Schnabel, H. and Schnabel, R. (1994). Genesis of an organ: molecular analysis of the *pha-1* gene. *Development* **120**, 3005-3017.
- Gu, W., Schneider, J. W., Condorelli, G., Kaushal, S., Mahdavi, V. and Nadal-Ginard, B. (1993). Interaction of myogenic factors and the retinoblastoma protein mediates muscle cell commitment and differentiation. *Cell* **72**, 309-324.
- Haas, A. L. and Siepmann, T. J. (1997). Pathways of ubiquitin conjugation. *FASEB J.* **11**, 1257-1268.
- Harbour, J. W. and Dean, D. C. (2000). The Rb/E2F pathway: expanding roles and emerging paradigms. *Genes Dev.* **14**, 2393-2409.
- Hill, A. A., Hunter, C. P., Tsung, B. T., Tucker-Kellogg, G. and Brown, E. L. (2000). Genomic analysis of gene expression in *C. elegans*. *Science* **290**, 809-812.

- Horner, M. A., Quintin, S., Domeier, M. E., Kimble, J., Labouesse, M. and Mango, S. E. (1998). *pha-4*, an HNF-3 homolog, specifies pharyngeal organ identity in *Caenorhabditis elegans*. *Genes Dev.* **12**, 1947-1952.
- Hsieh, J. K., Fredersdorf, S., Kouzarides, T., Martin, K. and Lu, X. (1997). E2F1-induced apoptosis requires DNA binding but not transactivation and is inhibited by the retinoblastoma protein through direct interaction. *Genes Dev.* **11**, 1840-1852.
- Huang, L. S., Tzou, P. and Sternberg, P. W. (1994). The *lin-15* locus encodes two negative regulators of *Caenorhabditis elegans* vulval development. *Mol. Biol. Cell* **5**, 395-411.
- Huang, L., Kinnucan, E., Wang, G., Beaudenon, S., Howley, P. M., Huijbregtse, J. M. and Pavletich, N. P. (1999). Structure of an E6AP-UbcH7 complex: insights into ubiquitination by the E2-E3 enzyme cascade. *Science* **286**, 1321-1326.
- Huibregtse, J. M., Scheffner, M., Beaudenon, S. and Howley, P. M. (1995). A family of proteins structurally and functionally related to the E6-AP ubiquitin-protein ligase. *Proc. Natl. Acad. Sci. USA* **92**, 5249.
- Ishida, S., Huang, E., Zuzan, H., Spang, R., Leone, G., West, M. and Nevins, J. R. (2001). Role for E2F in control of both DNA replication and mitotic functions as revealed from DNA microarray analysis. *Mol. Cell Biol.* **21**, 4684-4699.
- Joazeiro, C. A. and Weissman, A. M. (2000). RING finger proteins: mediators of ubiquitin ligase activity. *Cell* **102**, 549-552.
- Jones, D., Crowe, E., Stevens, T. A. and Candido, E. P. (2002). Functional and phylogenetic analysis of the ubiquitylation system in *Caenorhabditis elegans*: ubiquitin-conjugating enzymes, ubiquitin-activating enzymes, and ubiquitin-like proteins. *Genome Biol.* **3**, RESEARCH0002.
- Kaelin, W. G., Jr (1999). Functions of the retinoblastoma protein. *BioEssays* **21**, 950-958.
- Lu, X. and Horvitz, H. R. (1998). *lin-35* and *lin-53*, two genes that antagonize a *C. elegans* Ras pathway, encode proteins similar to Rb and its binding protein RbAp48. *Cell* **95**, 981-991.
- Luo, R. X., Postigo, A. A. and Dean, D. C. (1998). Rb interacts with histone deacetylase to repress transcription. *Cell* **92**, 463-473.
- Maduro, M. and Pilgrim, D. (1995). Identification and cloning of *unc-119*, a gene expressed in the *Caenorhabditis elegans* nervous system. *Genetics* **141**, 977-988.
- Magnaghi-Jaulin, L., Groisman, R., Naguibneva, I., Robin, P., Lorain, S., le Villain, J. P., Troalen, F., Trouche, D. and Harel-Bellan, A. (1998). Retinoblastoma protein represses transcription by recruiting a histone deacetylase. *Nature* **391**, 601-605.
- Mango, S. E., Lambie, E. J. and Kimble, J. (1994). The *pha-4* gene is required to generate the pharyngeal primordium of *Caenorhabditis elegans*. *Development* **120**, 3019-3031.
- Markey, M. P., Angus, S. P., Strobeck, M. W., Williams, S. L., Gunawardena, R. W., Aronow, B. J. and Knudsen, E. S. (2002). Unbiased analysis of RB-mediated transcriptional repression identifies novel targets and distinctions from E2F action. *Cancer Res.* **62**, 6587-6597.
- Martinez-Noel, G., Muller, U. and Harbers, K. (2001). Identification of molecular determinants required for interaction of ubiquitin-conjugating enzymes and RING finger proteins. *Eur. J. Biochem.* **268**, 5912-5919.
- Mello, C. and Fire, A. (1995). DNA transformation. *Methods Cell Biol.* **48**, 451-482.
- Mohler, W. A., Simske, J. S., Williams-Masson, E. M., Hardin, J. D. and White, J. G. (1998). Dynamics and ultrastructure of developmental cell fusions in the *Caenorhabditis elegans* hypodermis. *Curr. Biol.* **8**, 1087-1090.
- Morris, E. J. and Dyson, N. J. (2001). Retinoblastoma protein partners. *Adv. Cancer Res.* **82**, 1-54.
- Muller, H., Bracken, A. P., Vernell, R., Moroni, M. C., Christians, F., Grassilli, E., Prosperini, E., Vigo, E., Oliner, J. D. and Helin, K. (2001). E2Fs regulate the expression of genes involved in differentiation, development, proliferation, and apoptosis. *Genes Dev.* **15**, 267-285.
- Nevins, J. R. (2001). The Rb/E2F pathway and cancer. *Hum. Mol. Genet.* **10**, 699-703.
- Nielsen, S. J., Schneider, R., Bauer, U. M., Bannister, A. J., Morrison, A., O'Carroll, D., Firestein, R., Cleary, M., Jenuwein, T., Herrera, R. E. et al. (2001). Rb targets histone H3 methylation and HP1 to promoters. *Nature* **412**, 561-565.
- Ohtani, K., DeGregori, J. and Nevins, J. R. (1995). Regulation of the cyclin E gene by transcription factor E2F1. *Proc. Natl. Acad. Sci. USA* **92**, 12146-12150.
- Okkema, P. G., Harrison, S. W., Plunger, V., Aryana, A. and Fire, A. (1993). Sequence requirements for myosin gene expression and regulation in *Caenorhabditis elegans*. *Genetics* **135**, 385-404.
- Pickart, C. M. (2001). Ubiquitin enters the new millennium. *Mol. Cell* **8**, 499-504.
- Portereiko, M. F. and Mango, S. E. (2001). Early morphogenesis of the *Caenorhabditis elegans* pharynx. *Dev. Biol.* **233**, 482-494.
- Schnabel, H. and Schnabel, R. (1990). An organ-specific differentiation gene, *pha-1*, from *Caenorhabditis elegans*. *Science* **250**, 686-688.
- Schulze, A., Zeffass, K., Spitkovsky, D., Middendorp, S., Berges, J., Helin, K., Jansen-Durr, P. and Henglein, B. (1995). Cell cycle regulation of the cyclin A gene promoter is mediated by a variant E2F site. *Proc. Natl. Acad. Sci. USA* **92**, 11264-11268.
- Sellers, W. R., Novitsch, B. G., Miyake, S., Heith, A., Otterson, G. A., Kaye, F. J., Lassar, A. B. and Kaelin, W. G., Jr (1998). Stable binding to E2F is not required for the retinoblastoma protein to activate transcription, promote differentiation, and suppress tumor cell growth. *Genes Dev.* **12**, 95-106.
- Sherr, C. J. (1996). Cancer cell cycles. *Science* **274**, 1672-1677.
- Shih, H. H., Tevosian, S. G. and Yee, A. S. (1998). Regulation of differentiation by HBPI, a target of the retinoblastoma protein. *Mol. Cell Biol.* **18**, 4732-4743.
- Simmer, F., Tijsterman, M., Parrish, S., Koushika, S. P., Nonet, M. L., Fire, A., Ahringer, J. and Plasterk, R. H. (2002). Loss of the putative RNA-directed RNA polymerase RRF-3 makes *C. elegans* hypersensitive to RNAi. *Curr. Biol.* **12**, 1317-1319.
- Singh, P., Coe, J. and Hong, W. (1995). A role for retinoblastoma protein in potentiating transcriptional activation by the glucocorticoid receptor. *Nature* **374**, 562-565.
- Solari, F. and Ahringer, J. (2000). NURD-complex genes antagonise Ras-induced vulval development in *Caenorhabditis elegans*. *Curr. Biol.* **10**, 223-226.
- Strober, B. E., Dunaief, J. L., Guha, S. and Goff, S. P. (1996). Functional interactions between the hBRM/hBRG1 transcriptional activators and the pRB family of proteins. *Mol. Cell Biol.* **16**, 1576-1583.
- Sulston, J. E. and Hodgkin, J. (1988). Methods. In *The nematode Caenorhabditis elegans* (ed. W. B. Wood and the Community of *C. elegans* Researchers), pp. 587-606. Cold Spring Harbor, NY: Cold Spring Harbor Laboratory Press.
- Sulston, J. E. and Horvitz, H. R. (1977). Post-embryonic cell lineages of the nematode, *Caenorhabditis elegans*. *Dev. Biol.* **56**, 110-156.
- Tevosian, S. G., Shih, H. H., Mendelson, K. G., Sheppard, K. A., Paulson, K. E. and Yee, A. S. (1997). HBPI: a HMG box transcriptional repressor that is targeted by the retinoblastoma family. *Genes Dev.* **11**, 383-396.
- Thomas, D. M., Carty, S. A., Piscopo, D. M., Lee, J. S., Wang, W. F., Forrester, W. C. and Hinds, P. W. (2001). The retinoblastoma protein acts as a transcriptional coactivator required for osteogenic differentiation. *Mol. Cell* **8**, 303-316.
- Thomas, J. H. and Horvitz, H. R. (1999). The *C. elegans* gene *lin-36* acts cell autonomously in the *lin-35* Rb pathway. *Development* **126**, 3449-3459.
- Tong, H., Hateboer, G., Perrakis, A., Bernards, R. and Sixma, T. K. (1997). Crystal structure of murine/human Ubc9 provides insight into the variability of the ubiquitin-conjugating system. *J. Biol. Chem.* **272**, 21381-21387.
- Townsend, F. M., Aristarkhov, A., Beck, S., Hershko, A. and Ruderman, J. V. (1997). Dominant-negative cyclin-selective ubiquitin carrier protein E2-C/UbcH10 blocks cells in metaphase. *Proc. Natl. Acad. Sci. USA* **94**, 2362-2367.
- Tsai, K. Y., Hu, Y., Macleod, K. F., Crowley, D., Yamasaki, L. and Jacks, T. (1998). Mutation of E2F-1 suppresses apoptosis and inappropriate S phase entry and extends survival of Rb-deficient mouse embryos. *Mol. Cell* **2**, 293-304.
- Ulrich, H. D. (2003). Protein-protein interactions in an E2-RING finger complex. Implications for ubiquitin-dependent DNA damage repair. *J. Biol. Chem.* **278**, 7051-7058.
- von Zelewsky, T., Palladino, F., Brunschwig, K., Tobler, H., Hajnal, A. and Muller, F. (2000). The *C. elegans* Mi-2 chromatin-remodelling proteins function in vulval cell fate determination. *Development* **127**, 5277-5284.
- Wang, C., Deng, L., Hong, M., Akkaraju, G. R., Inoue, J. and Chen, Z. J. (2001). TAK1 is a ubiquitin-dependent kinase of MKK and IKK. *Nature* **412**, 346-351.
- Weissman, A. M. (2001). Themes and variations on ubiquitylation. *Nat. Rev. Mol. Cell Biol.* **2**, 169-178.
- Wiggan, O., Taniguchi-Sidle, A. and Hamel, P. A. (1998). Interaction of the pRB-family proteins with factors containing paired-like homeodomains. *Oncogene* **16**, 227-236.
- Yamanaka, A., Hatakeyama, S., Kominami, K., Kitagawa, M.,

- Matsumoto, M. and Nakayama, K.** (2000). Cell cycle-dependent expression of mammalian E2-C regulated by the anaphase-promoting complex/cyclosome. *Mol. Biol. Cell* **11**, 2821-2831.
- Zhang, H. S., Gavin, M., Dahiya, A., Postigo, A. A., Ma, D., Luo, R. X., Harbour, J. W. and Dean, D. C.** (2000). Exit from G1 and S phase of the cell cycle is regulated by repressor complexes containing HDAC-Rb-hSWI/SNF and Rb-hSWI/SNF. *Cell* **101**, 79-89.
- Zheng, N., Wang, P., Jeffrey, P. D. and Pavletich, N. P.** (2000). Structure of a c-Cbl-UbcH7 complex: RING domain function in ubiquitin-protein ligases. *Cell* **102**, 533-539.